3.34±1.42pT/mであり、２群間で統計学的有意差（$p<0.05$）を認めた。

D．考察

慢性めまい感の発現機序の一つに、大脳聴覚野の機能異常が関与することが示唆された。慢性めまい患者でみられた聴覚誘発磁界上の回転性電流異常は、側頭葉てんかん間歇期にみられる回転性電流異常に酷似していることから、てんかんに類似した異常電気放電が回転性電流を出現させている可能性が考えられた。

E．参考文献

1) P. Sloane, D. Blazer, L.K. George . Dizziness in a community elderly population. J.Am.Geriatr.Soc. 37:101-108,1989.

2) N.R. Colledge, J.A. Wilson, C.C.A. Macintype, W. J. Maclennan. The prevalence and characteristics of dizziness in an elderly community. Age & Ageing 23: 117-120, 1994.

3) W. Penfield W, H. Jasper: Epilepsy and the functional anatomy of the human brain. Boston, Little, Brown, 1954

4) A. Kandori., H. Oe, K. Miyashita, H. Date, N. Yamada, H. Naritomi, Y. Chiba, M. M. Murakami, T. Miyashita, K. Tsukada. Visualization method of spatial interictal discharges in temporal epilepsy patients by using magnetoencephalogram. Med. Biol. Eng. Comput. 40(3): 327-331, 2002

Patients		Complications	MRI findings
Age	Gender		
67	F	hyperlipidemia	no abnormality
56	F	deep vein thrombosis of legs	no abnormality
78	F	hyperlipidemia, chronic hepatitis	no abnormality
68	F	hypothyroidism	no abnormality
69	F	hypertension	no abnormality
58	M	hypertension	no abnormality
84	F	cervical spondylosis, hypertension	no abnormality
70	M	cerebral infarction	no abnormality
68	F	hypertension, chronic hepatitis	small infarcts in the deep white matters
59	M	diabetes mellitus	no abnormality
79	F	cerebral infarction, hyperlipidemia	small infarcts in the putamen
74	M	cervical spondylosis, diabetes mellitus	small infarcts in the deep white matters
60	M	cervical spondylosis, hypertension	no abnormality
71	M	cervical spondylosis, hypertension	no abnormality

表１　慢性めまい症例１４例の内訳

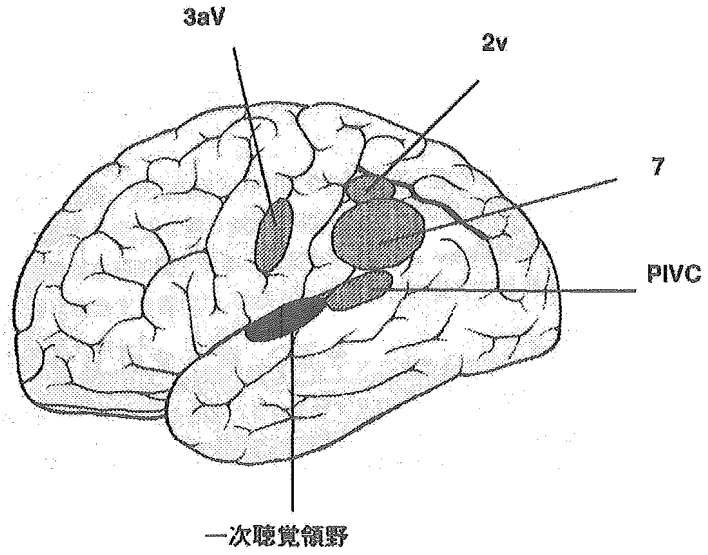

図１　前庭中枢（3aV, 2v, 7, PIVC)と一次聴覚領野

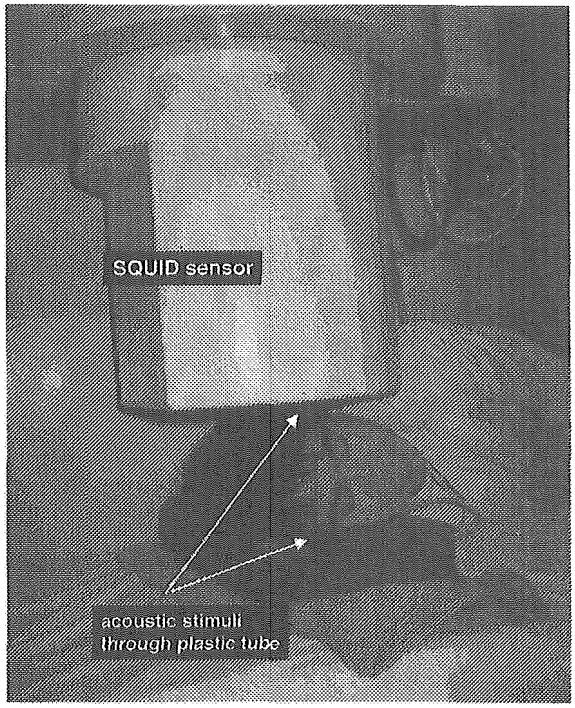

図２　日立MC-6400型生体磁気計測装置

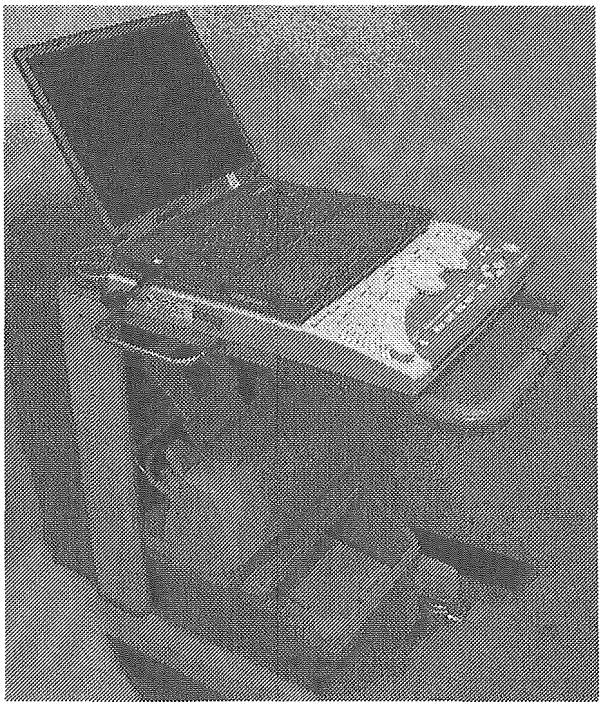

図３　日本光電Neuropack μ刺激信号発生装置

図４　正常例

図４－１
左側頭部記録でのAEFs
（右耳に聴覚刺激と
左耳にmasking sound）

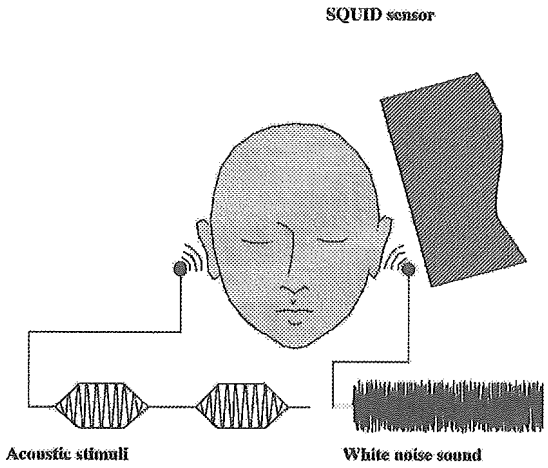

図４－２
左側頭部記録での
AEFsのN100m波形

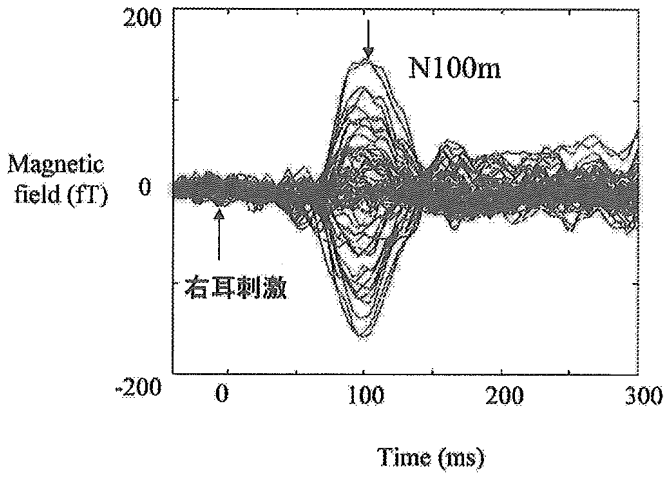

図４－３
AEFsのN100m成分の
current-arrow map

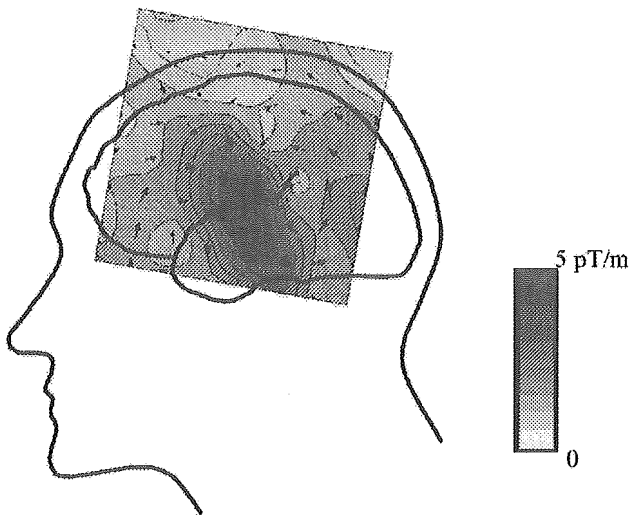

図５　慢性めまい例

図５－１
左側頭部記録でのAEFs
（右耳に聴覚刺激と
左耳にmasking sound）

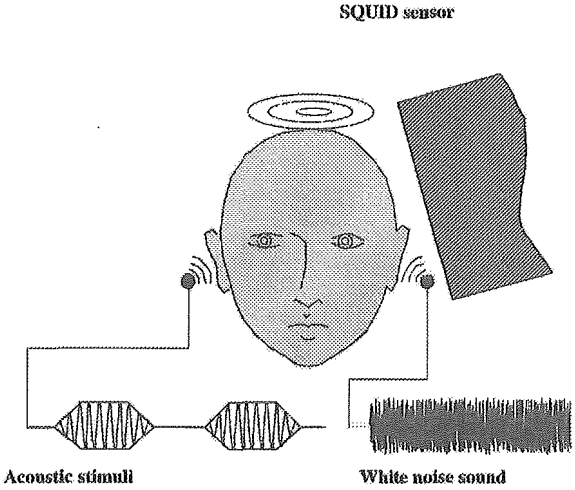

図５－２
左側頭部記録での
AEFsのN100m波形

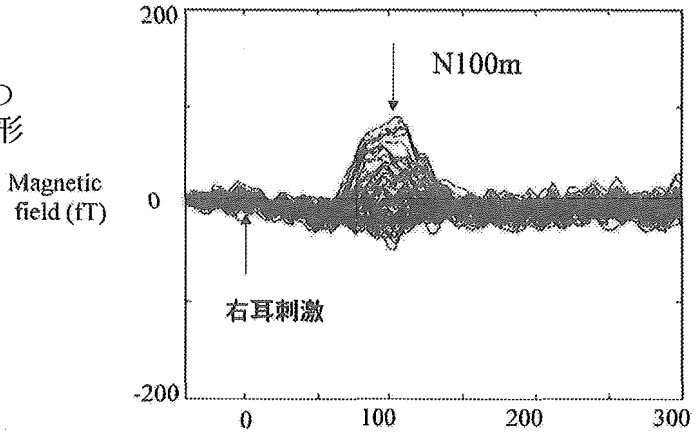

図５－３
AEFsのN100m成分の
current-arrow map

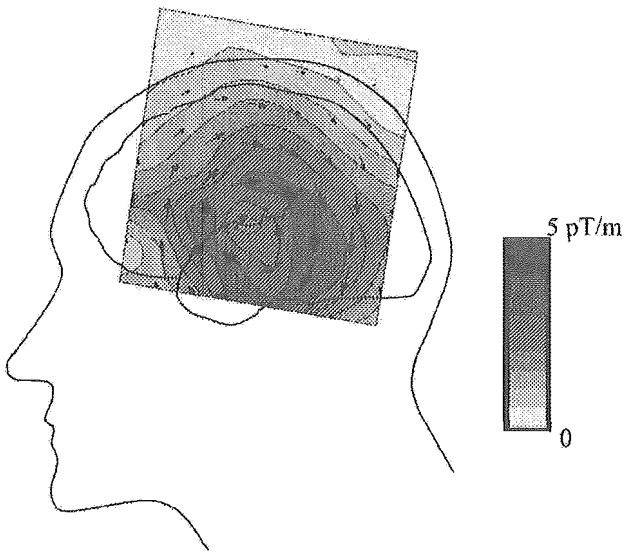

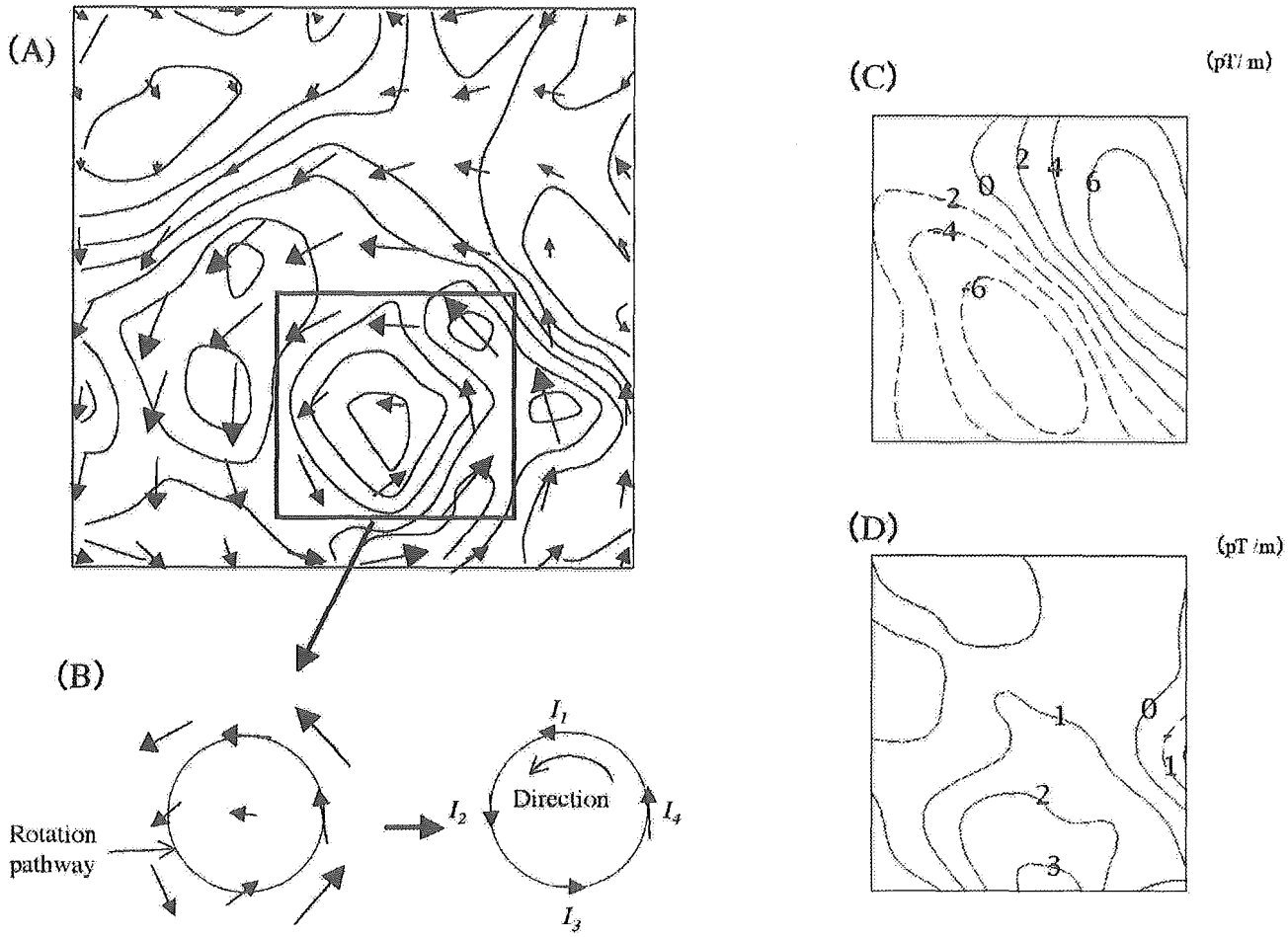

$$d\,I\,rot = I_1 + I_2 + I_3 + I_4$$

図６　電流アローマップの定量

図７　大脳皮質とcurrent-arrowの解剖学的位置関係

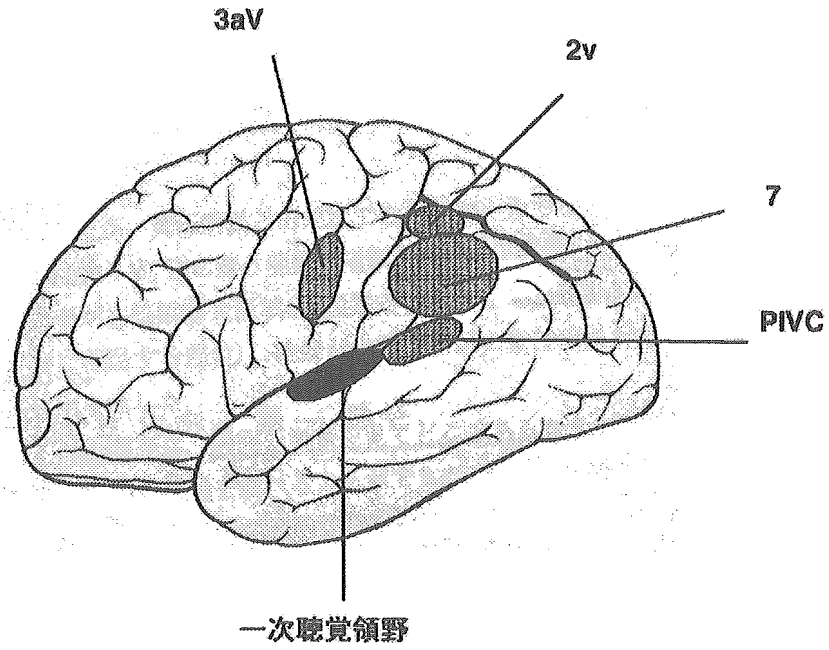

図７－１　一次聴覚野と前庭中枢の位置

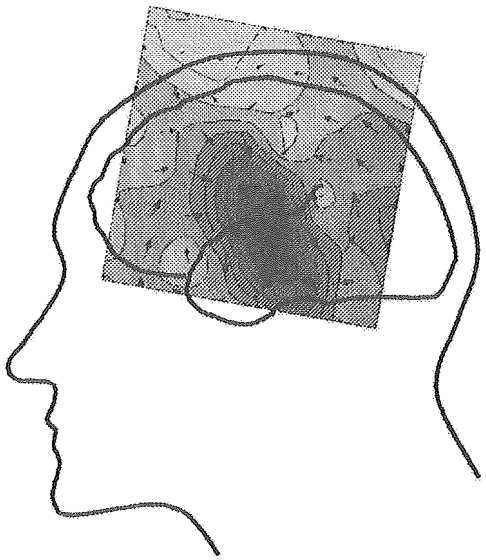

図７－２　正常例のcurrent-arrow map

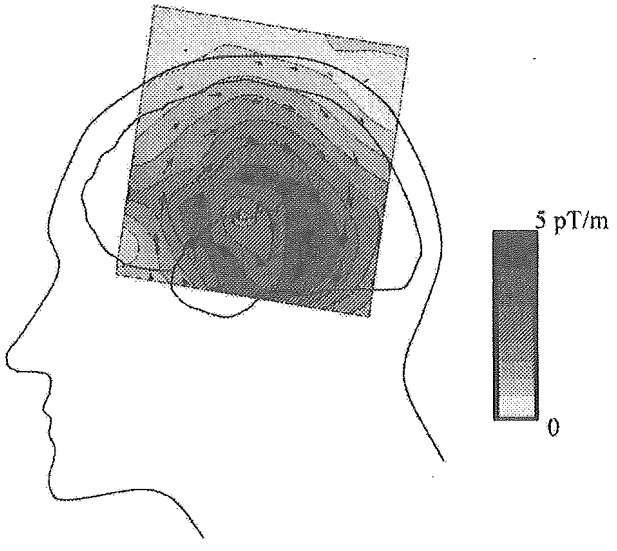

図７－３　慢性めまい例のcurrent-arrow map

Patients with chronic dizziness	
Grade of dizziness	*d I rot*
II	2.04
II	2.04
III	2.46
III	3.49
IV	4.18
III	2.33
IV	5.17
III	2.33
I	1.92
IV	4.86
IV	5.66
II	2.69
III	2.07
IV	5.43

表２　各症例ごとの自覚的ふらつきスケールと*d I rot*

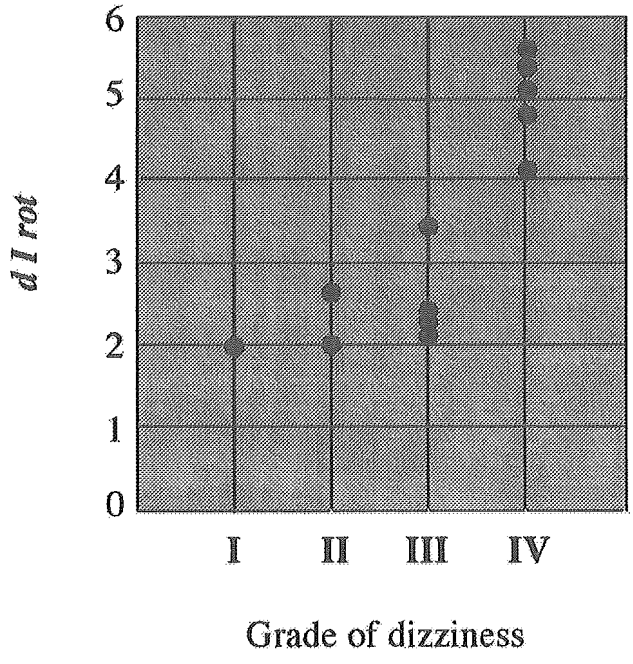

図８　自覚的ふらつきスケールと*d I rot*の関係

厚生科学研究費補助金（21 世紀型医療開拓推進研究事業）

分担研究報告書

Visualization method of spatial interictal discharges in temporal epilepsy patients by using magnetoencephalogram

[1]Akihiko Kandori, [2]Hiroshi Oe, [2]Kotaro Miyashita, [2]Hiroshi Date, [2]Naoaki Yamada, [2]Hiroaki Naritomi, [2]Yoshihide Chiba, [3]Masahiro Murakami, [1]Tsuyoshi Miyashita, and [1]Keiji Tsukada

[1]Central Research Laboratory, Hitachi, Ltd., 1-280 Higashi-koigakubo, Kokubunji-shi, Tokyo 185-8601, Japan

[2] National Cardiovascular Center, 5-7-1 Fujishirodai, Suita, Osaka 565-8565, Japan

[3] Instruments, Hitachi, Ltd., 882 Ichige, Hitachinaka-shi, Ibaraki 312-8504, Japan

Medical & Biological Engineering & Computing vol. 39-1, pp. 21-28, 2001

Abstract

The aim of our study was to develop a method for investigating how interictal epileptic discharges in temporal epilepsy patients are activated spatially. The activity was measured using magnetoencephalography (MEG). The MEG data were used to produce a current-arrow map, which reflects the topographic distribution of the electrical current, for each peak epileptic waveform. We obtained a large current distribution, which appeared to be contained in the limbic structure, in each temporal lobe. The large current orientation indicated two opposite directions. Furthermore, the

decrease of the maximum strength of the current arrow depending on the medication (e.g. the decease from 11 to 6 pT/m in left temporal lobe (contralateral stimuli)) suggested that we were able to use the discharge distributions to verify the efficacy of medication. Thus, our topographical visualization method could be a new strategy for diagnosis in temporal epilepsy patients.

Keywords: Magnetoencephalogram; Temporal epilepsy; Interictal discharge; Kindling phenomenon; Limbic structure, Current-arrow map

1. Introduction

Localization of the epileptogenic zone in patients with partial epilepsy is usually accomplished by magnetoencephalogram (MEG) recording (Baumgartner *et al.*, 2000; Brockhaus *et al.*, 1997; Forss *et al.*, 1995; Hari *et al.*, 1993; Kirchberger *et al.*, 1998; Knowlton *et al.*, 1997; Ko *et al.*, 1998; Nakasato *et al.*, 1994), especially in patients with neocortical partial epilepsy (Kirchberger *et al.*, 1998; Knowlton *et al.*, 1997; Nakasato *et al.*, 1994). However, in the case of temporal lobe epilepsy the localization has only been defined in 50% (Knowlton *et al.*, 1997) or 20% (Brockhaus *et al.*, 1997) because of interictal complex spikes. Such interictal spike activity mainly reflects the irritative zone, which in general is larger than the primary epileptogenic zone (Brockhaus *et al.*, 1997). On the other hand, the epileptic foci during seizures have been estimated (Brockhaus *et al.*, 1997; Forss *et al.*, 1995; Kirchberger *et al.*, 1998). However, head movement artifacts during seizures render reliable MEG recording almost impossible, and the seizures usually promote physical damage in the patients. Therefore, we have investigated the large spatial distribution, i.e. the transference phenomenon in the kindling effect, in interictal epileptic discharges in temporal epilepsy patients.

2. Materials and method

2.1 Subjects

Case 1: A 57-year-old man with a history of hypertension was hospitalized as an emergency case. While shopping, he had felt nausea, followed by syncope for only one minute. On admission, his consciousness had already become clear and he had no symptoms. Brain magnetic resonance imaging (MRI) showed degeneration and swelling of the hippocampus in the left medial temporal lobe. His electroencephalogram (EEG) indicated sharp waves in the left temporal area, and fluoro-2-deoxyglucose (^{18}F-FDG) positron emission tomography (PET) showed reduced ^{18}F-FDG up-take in that area. After administration of phenytoin, his EEG showed a decreasing paroxysmal discharge frequency.

Case 2: An 81-year-old man with a history of arrhythmia was hospitalized. His chief complaint was paroxysmal behavioral abnormality; for example, his body movement would stop suddenly and he would swing his right arm without consciousness for a few seconds. On admission, his consciousness was clear and his neurological signs showed no abnormality. His brain MRI demonstrated that the right hippocampus was larger than the left hippocampus. An EEG showed paroxysmal sharp waves with right-side dominance appearing in the temporoparietal area. The cerebral blood flow (CBF) distribution, obtained using hexamethyl-propyleneamine oxime single photon emission computed tomography (^{99m}Tc-HMPAO SPECT), had a normal pattern.

Case 3: A 61 year-old female, who had a history of hypertension, hyperlipidemia, and diabetes mellitus, was hospitalized. Her chief complaint was transient disorientation regarding people's faces, times, and dates. On admission, her consciousness was alert and her cognitive function was normal, as indicated by a score of 30 on the Mini-Mental State Examination (MMSE) (from a

possible score of 30) and a total IQ of 63 from the Wechsler Adult Intelligence Scale – Revised (WAIS-R) test. The higher cortical function showed no abnormality, and the awake and sleep EEGs demonstrated no paroxysmal discharge. Although her brain MRI showed no abnormality, a brain ^{99m}Tc-HMPAO SPECT image showed decreased cerebral blood flow in the right temporal lobe.

2.2. MEG measurements

We measured spontaneous MEGs and auditory evoked magnetic fields (AEMFs) by using a SQUID (superconducting quantum interference device) system (MC-6400, Hitachi, Ltd.) with a 64-coaxial gradiometer (Kandori *et al.*, 2001). This system was installed in a magnetically shielded room (MSR) with a double mumetal layer. The sensor array in the system is an 8x8 matrix on a flat plane with a pitch of 25 mm. Each sensor incorporates a first-order gradiometer that includes an 18-mm-diameter bobbin with a 50-mm-long baseline. The magnetic field sensitivities of all channels are below 20 fT $Hz^{-1/2}$.. The spontaneous MEG and AEMF were measured twice each for both hemispheres. The anatomical head position was adjusted by using four-coil indicators on an orbitomeatal basal (OM) line. After passing through a bandpass filter (0.1-50 Hz), notch filter (50 Hz), and amplifier circuit, the spontaneous MEG signals (2 minutes) were digitized at 1 kHz and the AEMF signals (8 minutes) were digitized at 250 Hz by a computer. Although we could not measure both hemispheres at the same time because of the flat measurement plane, it was sufficient to detect signals from the temporal lobe, which could be fitted by the flat plane.

2.3. Signal analysis

To detect only the epileptic waveform, we subtracted the magnetocardiogram signals deriving

from the patients' hearts from the spontaneous MEG signals. Then, in the same manner as for EEG epilepticform analysis (Kobayashi *et al.*, 2001; Kunieda *et al.*, 2000), we manually averaged the epileptic sharp waves to obtain a clear signal. We then compared the raw epileptic waveforms and the averaged waveforms to eliminate the influence of waveform distortion. To visualize the epileptic discharge current inside the brain two-dimensionally, we produced current-arrow maps by deriving the normal component (Bz) of the magnetic field[9].. Such current maps are useful for reviewing neural networks directly and topographically without dipole estimation, although the head sphere shape affects the current-arrow pattern. By using a current-arrow pattern with each epileptic discharge waveform, the averaged discharge could be visualized. For these measurements, informed consent was obtained from all patients.

3. Results

We measured MEG signals for the case-1 patient both before administration of phenytoin (Figs. 1, 2, and 3) and after (Fig. 4). Figure 1a shows the original spontaneous MEG signal in the left temporal lobe. We can see negative sharp waves and positive sharp waves. Furthermore, in the right temporal lobe (Fig. 1b), there were sharp waves of smaller magnitude than those in Fig. 1a, and the number of sharp waves in right temporal lobe (Fig. 1a) is smaller than that of sharp waves in left temporal lobe (Fig. 1b).

Figure 2 shows the averaged negative waveforms and positive waveforms for each temporal lobe in a sensor array. A distribution of negative and positive waveforms in left temporal lobe (a) is same in the sensor array, although a magnitude of the waveforms is different. On the other hand, channel in which a maximum waveform appears in right temporal lobe is different.

Figures 3d and a show the averaged negative waveforms and a current arrow map at the

peak in these waveforms, respectively. Figures 3e and b show the same results for the positive waveforms. The two maps of Figs. 3a and b indicate that the activity area in the left temporal lobe was the same for both waves, and that the orientations of the neural circuits were opposite. Figures 3c and f show a map at the N100m peak and the AEMF signals, respectively. In the map of Fig. 3c, we obtained a landmark of the auditory cortex. As a result, we found that the largest epileptic discharge occurred on the auditory cortex and that circular discharge currents spread to the front-temporal and middle-temporal areas. Furthermore, since small epileptic waveforms (Figs. 3j and k) in right temporal lobe can also be seen, the current-arrow maps (Figs. 3g, h, and i) may indicate that epileptic discharge currents appeared around the auditory cortex. The maximum strength of the current arrow of Fig. 3 was 11 (a), 15 (b), 12 (g), and 7 pT/m (h), respectively.

For comparison to illustrate the effect of administering phenytoin, Figs. 4 show current-arrow maps produced from the case-1 patient's MEG epileptic signals after medication. In the left temporal lobe (Figs. 4a and b), the expansions in the epileptic circular current were smaller than those of in Figs. 3a and b, and the main discharge currents remained on or near the auditory cortex. On the other hand, in the right temporal lobe (Figs. 4c and d) the magnitudes of the discharge currents throughout became smaller than those before medication. Furthermore, the main discharge currents appeared behind the auditory cortex, near the hippocampus. The maximum strength of the current arrow of Fig. 4 was 6 (a), 11 (b), 8 (g), and 6 pT/m (h), respectively. All of the strength was smaller than that before the medication.

In the case-2 patient (Figs. 5a and b), the spread currents appeared in the right hemisphere. However, epileptic waveforms were not seen in the left hemisphere. In the case-3 patient (Fig. 5c), weak epileptic discharge waveforms appeared only in the left hemisphere, although there were no paroxysmal discharges in the awake and sleep EEGs. A distribution of discharges also appeared throughout the whole left hemisphere.

4. Discussion

Our data indicate that an interictal temporal discharge has a wide distribution in the temporal area. In particular, in two cases out of three, the current orientation had two patterns, reflecting depolarization and repolarization in the paroxysmal membrane (Amzica and Neckelmann, 1999; Curtis and Avanzini, 2001)). The distribution suggests the existence of a kindling transference phenomenon in the limbic structure. This transference has been examined in adult cats (Akimoto and Yamaguchi, 1984; Racine *et al.*, 1972a; Racine *et al.*, 1972b; Sato *et al.*, 1980), showing that a connection in the limbic structure indicated a positive transference among the septum, the accumbens, the amygdala, the hippocampus, and the sylvian gyrus. In cases 1 and 2, swelling and ambulance size of the hippocampus were observed by MRI. Furthermore, small discharges still existed near the hippocampus in the right temporal lobe (Figs. 4c and d) after phenytoin medication. Therefore, in these cases temporal epileptic discharges may have propagated from the hippocampus as an origin. Especially in case 1, the efficacy of the phenytoin medication could be verified by the discharge distribution and the decrease of the maximum strength of the current arrow, as shown in Figs. 4a-d. As in our current study, the kindling effect has also been discussed for trigeminally triggered epileptic hemifacial convulsion, which is a rare clinical condition. In that case, abnormal impulsation in the trigeminal pathway might have caused kindling in the cortical motor face area. In contrast, the interictal temporal discharges we obtained in or near the hippocampus could have caused the kindling (projection and propagation) in the limbic structure.

Furthermore, the case-1 patient had epileptic discharges in both hemispheres, and the distributions in the left hemisphere were larger than those in the right. These discharge distributions may support Hari's data on mirror focus (Hari *et al.*, 1993), although we could not measure both

sides simultaneously. Mirror focus development has been investigated by using intermittent stimulation in animals (Mclntyre and Poulter, 2001; Racine *et al.*, 1972a; Racine *et al.*, 1972b). In these experiments, the most powerful contralateral transfer effects in the rat occurred between the two hippocampi (Racine *et al.*, 1972a). In our results, the negative waveforms (Fig. 1a) in the left temporal area may have transferred or projected to positive waveforms (Fig. 1b) in the right temporal lobe because both types of waveforms occurred in much larger numbers than the opposite waveforms. Therefore, in case 1, the observed contralateral discharge with small current-arrow patterns suggests a projection from primary discharge activities.

Large interictal electrical discharge distribution in temporal epilepsy patients could be visualized with current-arrow maps based on MEG measurement. Although the current-arrow maps have a feature to reflect a surface current distribution, it was suggested that the kindling effect in the limbic structure caused the large distribution in each hemisphere because the discharge propagated from hippocampus in the limbic structure.. In one patient (case 1), a small spread pattern, which reflects mirror projection, also occurred in the contralateral lobe. After anti-epileptic medication, the magnitude of the discharge decreased and the pattern became smaller. It can thus be concluded that topographic visualization based on MEG has the potential to help determine the causes and mechanisms of neurological disorders.

References

Akimoto H., and Yamauchi T., Textbook of epileptology: Iwasaki Gakujutsu Shuppansha Press (1984) 502- 510

Amzica F. and Neckelmann D., Membrane capacitance of cortical neurons and glia during sleep oscillations and spike-wave seizures, J. Neurophysiol. 82(5) (1999) 2731-2746

Baumgartner C., Pataraia E., Lindinger G. and Deecke L., Magnetoencephalography in focal epilepsy, Epilepsia 41 Suppl 3 (2000) S39-S47

Brockhaus A., Lehnertz K., Wienbruch C., Kowalik A., Burr W., Elbert T., Hoke M. and Elger C.E., Possibilities and limitations of magnetic source imaging of methohexital-induced epileptiform patterns in temporal lobe epilepsy patients, Electroencephalogr. Clin. Neurophysiol. 102 (1997) 423-436

de Curtis M. and Avanzini G., Interictal spikes in focal epileptogenesis, Prog. Neurobiol. 63(5) (2001) 541-567

Forss N., Mäkelä J.P., Keränen T. and Hari R., Trigeminally triggered epileptic hemifacial convulsions, NeuroReport 6, (1995) 918-920

Hari R., Ahonen A., Forss N., Granström M-L., Hämäläinen M., Kajola M., Knuutila J., Lounasmaa O.V., Mäkelä J.P., Paetau R., Salmelin R. and Simola J., Parietal epileptic mirror focus detected with a whole-head neuromagnetometer, NeuroReport 5, (1993) 45-48

Kandori A., Kanzaki H., Miyatake K., Hashimoto S., Itoh S., Tanaka N., Miyashita T. and Tsukada K., A method for detecting myocardial abnormality by using a total current-vector calculated from ST-segment deviation of a magnetocardiogram signal, Med. Biol. Eng. Comput. 39(1) (2001) 21-28

Kirchberger K., Schmitt H., Hummel C., Peinemann A., Pauli E., Kettenmann B. and Stefan H., Clonidine- and Methohexital-induced epileptiform discharges detected by magnetoencephalography (MEG) in patients with localization-related epilepsies, Epilepsia 39(10), (1998) 1104-1112

Knowlton R.C., Laxer K.D., Aminoff M.J., Roberts T.P.L., Wong S.T.C. and Rowley H.A., Magnetoencephalography in partial epilepsy: clinical yield and localization accuracy, Ann. Neurol.

42 (1997) 622-631

Ko D.Y., Kufta C., Scaffidi D. and Sato S., Source localization determined by magnetoencephalography in temporal lobe epilepsy: comparison with electrocorticography: technical case report, Neurosurgery 42(2), (1998) 414-422

Kobayashi K., Merlet I. and Gotman J., Separation of spikes from background by independent component analysis with dipole modeling and comparison to intracranial recording, Clin. Neurophysiol. 112 (2001) 405-413

Kunieda T., Ikeda .A, Nikuni N. Ohara S, Sadato A., Taki W., Hashimoto N. and Shibasaki H., Use of cavernous sinus EEG in the detection of seizure onset and spread in mesial temporal lobe epilepsy, Epilepsia 41(11) (2000) 1411-1419

Mclntyre D.C. and Poulter M.O, Kindling and the mirror focus, Int. Rev. Neurobiol. 45 (2001) 387-407

Nakasato N., Levesque M.F., Barth D.S., Baumgartner C., Rogers R.L. and Sutherling W.W., Comparison of MEG, EEG, and ECoG source localization in neocortical partial epilepsy in humans, Electroencephalogr. Clin. Neurophysiol. 171 (1994) 171-178

Racine R.J, Burnham W.M., Gartner J.G. and Levitan D., Modification of seizure activity by electrical stimulation. II. Motor seizure, Electroencephalogr. Clin. Neurophysiol. 32 (1972a) 281-294

Racine R.J., Gartner J.G. and Burnham W.M., Epileptiform activity and neural plasticity in limbic structures, Brain Res. 47 (1972b) 262-268

Sato M., Kindling, transference phenomenon between temporal cortex and limbic structure in cats, Adv. Physiol. Sci. 17 Pergamon Press (1980) 509-516

Figure captions

Fig. 1: Spontaneous MEG signals, with '*' indicating the averaged waveforms (upper indicators are for positive waveforms, lower indicators are for negative waveforms), for case 1 in the left temporal lobe (**a**) and right temporal lobe (**b**).

Fig. 2: Averaged negative and positive waveforms for left temporal lobe (**a**) and right temporal lobe (**b**) in a sensor array.

Fig. 3: **a**: Current-arrow map at the peak in the epileptic waveforms of **d**. **b**: Current-arrow map at the peak in the epileptic waveforms of **e**. **c**: Current-arrow map at N100m in the AEMF waveforms of **f**. **d**: Sixty-four averaged (52 times) negative epileptic waveforms. **e**: Sixty-four averaged (16 times) positive epileptic waveforms. **f**: AEMF waveforms. **g**: Current-arrow map at the peak in the epileptic waveforms of **j**. **h**: Current-arrow map at the peak in the epileptic waveforms of **k**. **i**: Current-arrow map at the peak at N100m in the AEMF waveforms of **l**. **j**: Sixty-four averaged (7 times) negative epileptic waveforms. **k**: Averaged (35 times) sixty-four positive epileptic waveforms. **l**: AEMF waveforms.

Fig. 4: Current-arrow maps for case 1 after phenytoin medication. In comparison with the maps obtained before medication, the current arrows changed to a narrower distribution.

Fig. 5: Current-arrow maps for case 2 (**a**,**b**), and case 3 (**c**). **a**,**b**: Two epileptic patterns were measured only in the right temporal lobe. **c**: One epileptic pattern was measured only in the left temporal lobe.